Turkish Journal of Electrical Engineering & Computer Sciences

http://journals.tubitak.gov.tr/elektrik/

Research Article

Turk J Elec Eng & Comp Sci
(2015) 23: 931 – 944

doi:10.3906/elk-1210-4

A comparative study of denoising sEMG signals

Ulvi BAŞPINAR[1], Volkan Yusuf ŞENYÜREK[1], Barış DOĞAN[2,*], Hüseyin Selçuk VAROL[1]

[1]Electronics and Computer Education Department, Technical Education Faculty, Marmara University, Göztepe Campus, Kadıköy, İstanbul, Turkey

[2]Mechatronics Education Department, Technical Education Faculty, Marmara University, Göztepe Campus, Kadıköy, İstanbul, Turkey

Received: 01.10.2012 • **Accepted/Published Online:** 17.04.2013 • **Printed:** 10.06.2015

Abstract: Denoising of surface electromyography (sEMG) signals plays a vital role in sEMG-based mechatronics applications and diagnosis of muscular diseases. In this study, 3 different denoising methods of sEMG signals, empirical mode decomposition, discrete wavelet transform (DWT), and median filter, are examined. These methods are applied to 5 different levels of noise-added synthetic sEMG signals. For the DWT-based denoising technique, 40 different wavelet functions, 4 different threshold-selection-rules, and 2 threshold-methods are tested iteratively. Three different window-sized median filters are applied as well. The SNR values of denoised synthetic signals are calculated, and the results are used to select DWT and median filter method parameters. Finally, 3 methods with the optimum parameters are applied to the real sEMG signal acquired from the flexor carpi radialis muscle and the visual results are presented.

Key words: Surface electromyography, sEMG, empirical mode decomposition, empirical mode decomposition, denoising, wavelet, median filter

1. Introduction

Analysis of electromyography (EMG) signals acquired from skin surface electrodes over muscles has important uses in various applications including neurological diagnosis, neuromuscular and psychomotor research, sports medicine, prosthetics, rehabilitation, and robot limb control [1–5]. Nevertheless, EMG signal acquisition from the body surface is influenced by undesired effects mostly derived from electrodes, cables, data amplification and acquisition devices, power lines, and even the body itself. These effects are called artifacts, interference, and noise in general, and they can easily ruin the resolution and form of biomedical recordings [6,7].

Conventional filtering techniques such as low-pass, high-pass, and band-pass can be used for reducing line interference, thermal noise, etc. Choosing high-quality electrodes and equipment can also reduce undesired artifacts [8]. These techniques are useful when the noise spectrum is known and separable from the original signal. However, conventional techniques cannot remove random noise such as impulse within the active EMG signal spectrum band (20–500 Hz), and they can smooth the source EMG signal edges [9,10].

Recently, novel methods such as wavelet and empirical mode decomposition (EMD) have been successfully applied to remove noise from sEMG signals [11–14]. EMD, which has a wide application area in science and engineering, is a new signal decomposition method for analyzing data [15,16].

Wavelets are a popular method for attaining information from different kinds of signal sources. They are

*Correspondence: baris@marmara.edu.tr

preferred in compression/decompression algorithms because they preserve the original information. They are also used in feature extraction [17,18]. Median filtering is a nonlinear digital filtering technique for removing high-frequency noise, particularly that which is derived from signal acquisition [19]. Both EMD and wavelets are popular in denoising biomedical signals. There are some studies that compared EMD-based denoising and wavelet-based denoising on biomedical signals like ECG [20] and EEG [21]. However, they are not directly intended to investigate denoising sEMG signals while comparing the effect of median filtering.

In this study, 5 different levels of noise are added to synthetic sEMG signals. An online database is preferred for the synthetic sEMG signal source in order to allow the denoising results be tested and to make further studies using the same signals as a source. EMD, DWT, and median filter are applied to the noisy synthetic sEMG signals. Signal-to-noise ratio (SNR) values are calculated to be able to select optimum filter parameters such as window size for the median, wavelet functions, threshold methods, and rules. Finally, denoising methods with optimum parameters are applied to the real sEMG signals and the process results are presented as well.

2. Materials and methods

This study was performed on 2 different signal sources:

- synthetic sEMG signals taken from [22] and shown in Figure 1,
- real sEMG signals acquired from the flexor carpi radialis muscle as shown in Figure 2.

A specially designed homemade EMG amplifier was used in the preamplification of real sEMG signals. A precision instrumentation amplifier (IC AD8295) was chosen in the schematic as shown in Figure 3, and the gain was set to 200 by choosing RG resistance as 250 Ω. In order to suppress higher frequencies, a two-pole Sallen-Key low-pass filter was connected at the output of the amplifier, which had a cutoff frequency of 500 Hz. The measurement system was powered by a 12-V, 7.2-Ah rechargeable battery to avoid line interferences. The filtering frequency of the low-pass filter could be adjusted by changing R1, R2 resistors and C1, C2 capacitances. The electrodes used in the study were Ag/AgCl bipolar passive disposable electrodes (Myotronics Inc.) which were 1 mm in diameter with an interelectrode distance of 20 mm. After preamplification, the real sEMG signal was sampled with 4 kHz at 16-bit resolution with the help of a USB data acquisition card (I/O Tech Comp.). An overall view of the sEMG measurement environment and the equipment can be seen in Figure 4.

2.1. EMD algorithm and EMD-based denoising

EMD is a method first introduced by [23]. In this method, the complex data are decomposed into a finite and often small number of oscillatory components, called intrinsic mode functions (IMFs). An IMF must provide two conditions:

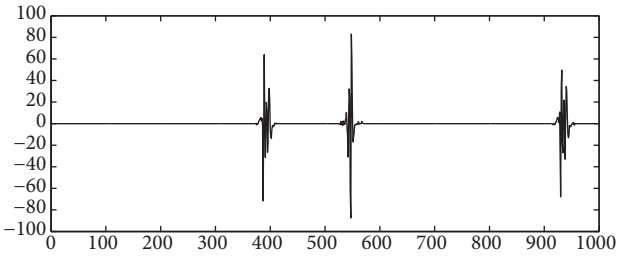

Figure 1. Synthetic sEMG signal.

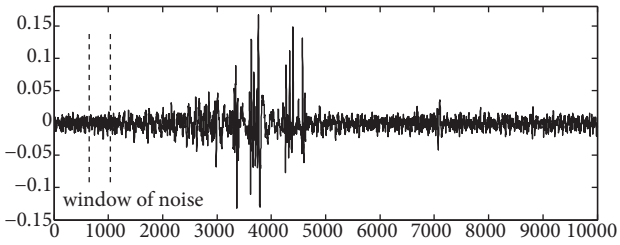

Figure 2. Real sEMG signal.

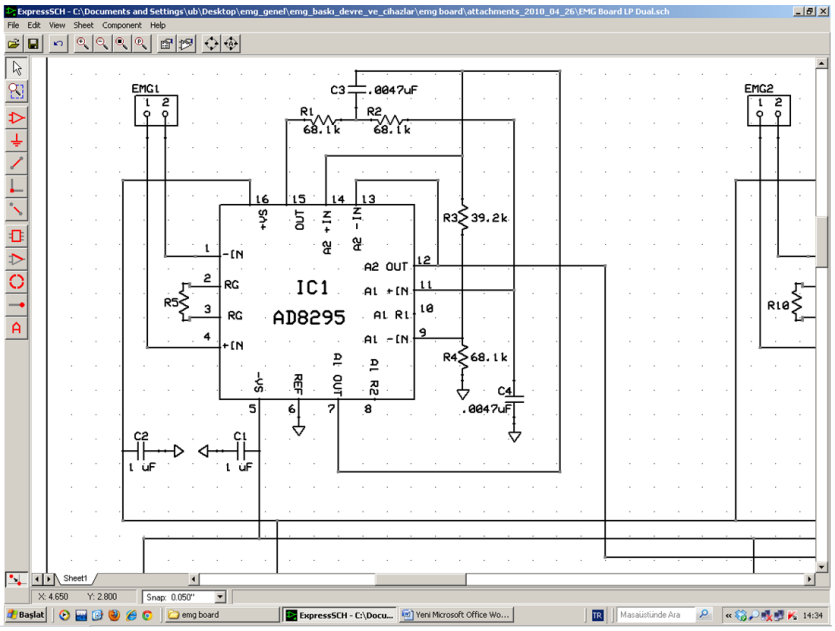

Figure 3. The schematic of the sEMG amplifier circuit.

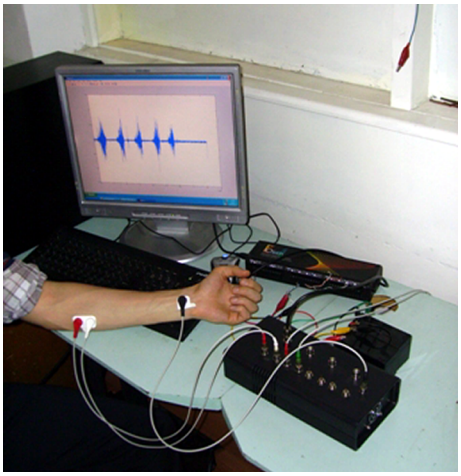

Figure 4. A picture of the real sEMG signal measurement.

i. In the whole data set, the number of extreme and zero crossings must be equal, or differ at most by one;

ii. At any point, the mean value of the envelope defined by the local maxima and the local minima must be zero.

IMFs can be found by a process called shifting. The shifting process, adopted from [12], involves the steps below.

a) $X(t)$ is a variable and is set to the original signal $S(t)$ to be analyzed.

b) Find all minima and maxima of the signal $X(t)$.

c) Produce the upper envelope (UE) and lower envelope (LE) using the minima and maxima that are found in step 2 (Figure 5a).

d) Calculate the mean of the envelopes $[ME = (UE + LE)/2]$ (Figure 5b).

e) Compute the candidate $IMF(h)$ $[h = x(t) - ME]$ (Figure 5c).

f) Test the candidate IMF for whether it fulfills the conditions of being an IMF or not. If not, assign h as $x(t)$ and go back to step 1, or assign h as IMF.

g) Calculate the mean squared error (MSE) of two consecutive IMFs. If the MSE is small enough to stop the condition $(\approx 10e-5)$ then stop the process; if not, the partial residue (r_k) is estimated as the difference between a previous partial residue $(r_k - 1)$ and $IMF(r_k = (r_k - 1) - IMF)(r_0 = S(t))$. Its content is then assigned to the variable $x(t)$ and the process goes back to step 2.

h) Carry on until the MSE is smaller than the stop condition or only one maximum is left.

i) When the shifting process is completed, the original signal $S(t)$ can be represented as in Eq. (1).

$$S(t) = \sum_{k=1}^{n} IMF_k + r_{final}, \tag{1}$$

where $S(t)$ is the original signal, r_{final} is the final residue, and n is the number of IMFs.

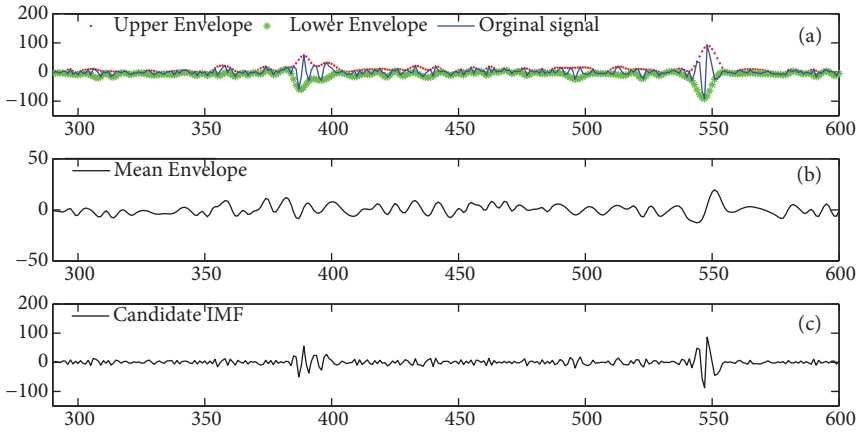

Figure 5. Illustration of the sifting processes: (a) the original signal (blue line), upper envelope (red dot-dashed line), lower envelope (green star-dashed line); (b) the mean envelope; (c) the difference between the original signal and mean envelope. This is still not an IMF, for it does not fulfill the conditions of being an IMF as mentioned before.

The EMD-based denoising technique consists of 3 levels. At the first level, a noisy signal is decomposed into IMFs. Secondly, each IMF signal is thresholded, and finally, all thresholded IMFs are reconstructed.

In this study, the soft-thresholding technique proposed in [24] was used with a universal threshold for removing Gaussian noise (t_i), as given in Eq. (2).

$$t_i = \varsigma_i(2\log(L))^{1/2} \tag{2}$$

$$\varsigma_i = med_i/0.6745 \tag{3}$$

Here, t_i is the threshold, ς_i is noise level of the ith IMF, and L is the size of the IMF.med_i represents the median absolute deviation of the ith IMF and is defined by Eq. (5).

$$u = Median\{IMF_i(t) \tag{4}$$

$$med_i = Median\{|IMF_i(t) - u|\} \tag{5}$$

The soft-thresholding method shrinks the IMF samples by t_i towards zero as shown in Eq. (6):

$$Y_i(t) = \begin{cases} IMF_i - t_i & \text{if} \quad IMF_i(t) \geq t_i \\ 0 & \text{if} \quad |IMF_i(t)| < t_i \\ IMF_i + t_i & \text{if} \quad IMF_i(t) \leq -t_i \end{cases}, \tag{6}$$

where Y_i denotes the denoised signal.

2.2. Discrete wavelet algorithm and discrete wavelet-based denoising

The discrete wavelet transform (DWT) [25,26] is a convenient way to represent and manipulate signals featuring sharp transients. It splits the signal into its "low-resolution" parts and a series of details at different resolutions. This process is described in terms of filter banks (Figure 6). In filter banks, the signals under analysis are divided into two components, S(n) and T(n), by digital filters L and H. L stands for the low-pass filter while H stands for the high-pass filter. For the signal reconstruction, the filtering process is simply reversed. One common application of the DWT is denoising, which has received considerable attention in the removal of noise in biomedical signals [27–31].

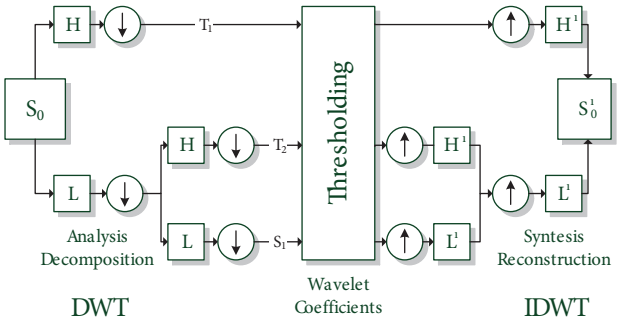

Figure 6. Typical DWT denoising application using filter banks.

The DWT-based denoising algorithm is based on three stages:

i. The DWT transforms of the signal,

ii. Thresholding the wavelet coefficients,

iii. Reconstruction of the denoised signal by using inverse wavelet transforms of the thresholded wavelet coefficients.

When additive white Gaussian noise (AWGN) is added to any signal $y(n)$, it can be represented by the summation of the original signal $s(n)$ and the noise $n(n)$, as shown in Eq. (7).

$$y(n) = s(n) + n(n) \tag{7}$$

After performing the wavelet transform, the result is found as in Eq. (8).

$$Y_{i,m} = S_{i,m} + N_{i,m} \tag{8}$$

In order to denoise the signal, a proper threshold must be defined after the wavelet decomposition process. Generally, four classical threshold deviation methods are used: universal threshold, SURE threshold, minimax threshold, and hybrid threshold.

The last step of the thresholding is the selection of the threshold type. There are two common ways to threshold the wavelet coefficient results. The first one is referred to as hard thresholding, which sets the coefficients whose absolute value are below the threshold level (λ) to zero.

$$Y_{i,m} = \begin{cases} Y_{i,m} & |Y_{i,m}| > \lambda \\ 0 & otherwise \end{cases} \tag{9}$$

The second one is called soft thresholding, and it is a continuous function that decreases the value of the signal by the threshold level. The denoised signal is reconstructed utilizing the process known as inverse transform, which is simply the reverse of the wavelet transform.

2.3. Median filtering

The main property of median filtering is to remove high frequency noise such as impulses while preserving the edges of the original signal form. It is very popular in acoustics and speech and signal processing, and today it is becoming popular in image processing, also called 2-dimensional signal processing.

Theoretically, if the 2 signals are $x(t), y(t) \Rightarrow$

$$median[x(t) + y(t)] \neq median[x(t)] + median[y(t)]. \tag{10}$$

This filter uses the sliding window method. While in process, the filter sorts the elements in the window, and if the window size is odd, it replaces the mid-value with the current value. Otherwise, it calculates the average of the two mid-values and replaces them with the current value. The window size should be defined in detail for there is a risk of losing the original signal form.

While $x(t) = \{v_0, v_1, v_2, \ldots, v_n\}$ is a sorted array,

$$median[x(t)] = \begin{cases} V_m & \Longleftrightarrow \quad m = \frac{n-1}{2}, nisodd \\ \frac{v_{k-1}+v_k}{2} & \Longleftrightarrow \quad k = \frac{n}{2}, niseven \end{cases}. \tag{11}$$

3. Results

This section is divided into two subsections. In the first section, the results for EMD- and DWT-based denoising and median filtering of the synthetic sEMG are discussed; in the second section, the results of the real sEMG are presented.

3.1. Denoising results of the synthetic sEMG signals

The performances of the denoising methods were compared according to the criteria of the SNR in dB as shown in Eq. (12):

$$SNR\,[dB] = 10log_{10}\frac{\sum_{n=1}^{N} x[n]^2}{\sum_{n=1}^{N} \left(\acute{x}[n] - x[n]\right)^2}, \tag{12}$$

where $x[n]$ denotes the synthetic signal and $\acute{x}[n]$ represents the denoised signal.

In order to observe the performances of the denoising techniques, AWGN was added to the synthetic signal at five different levels ($2dB$,$0dB$, $-2dB$, $-5dB$, and $-7dB$). The noise-adding process was realized in a MATLAB environment 30 times for each noise level and denoising techniques were performed on each of these generated noisy sEMGs separately.

The first step of the EMD-based denoising is selecting the window of noise. In this study, we assigned the window of noise covering 100 samples as shown in Figure 7. The noisy signals were then decomposed into their IMFs, as shown in Figure 8. The decomposed signals were thresholded, and the filtered IMFs were reconstructed as well. During the filtering and reconstruction processes, all derived IMFs and residues were used.

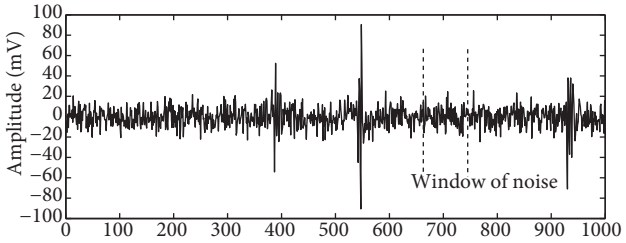

Figure 7. A –2 dB AWGN-added synthetic sEMG signal.

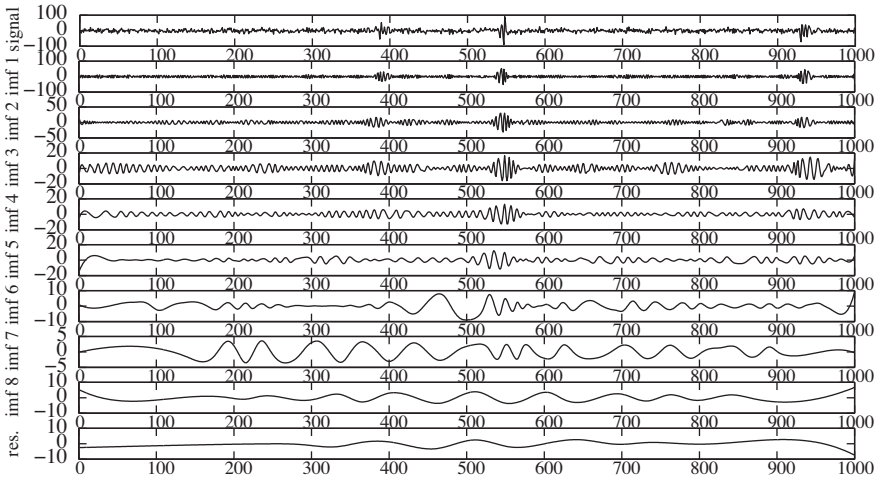

Figure 8. IMF signals of a noisy synthetic sEMG signal.

In DWT-based denoising, determining the wavelet function that gives the best SNR values is a very important issue. To do so, the following study was performed on all generated noisy sEMG signals individually. First, one wavelet was selected from among 40 different wavelets. Second, 4 different threshold selection rules (universal, minimax, SURE, hybrid) and the soft/hard threshold method were applied at the 8-level

decomposition. Last, the SNR values of noisy and denoised signals were recorded. These processes were repeated for all 40 wavelets. In Figure 9, the histograms of the wavelets whose SNR values are above the defined SNR thresholds are depicted. According to Figure 9, the optimum performance is provided with bior1.1, haar, and sym5 wavelets at $2dB$, $0dB$ and $-2dB$ noise levels while with sym4, sym8, coif2, and coif5 wavelets at $-5dB$ and $-7dB$ noise levels.

The comparison of threshold methods showed that the hard threshold method performs better with less noisy signals while the soft threshold method performs better with more noisy signals. The study also showed that minimax and SURE selection rules are better than the universal and hybrid selection rules in denoising of sEMG signals. The wavelet function, threshold rule, and threshold selection criteria that are used in the calculation of mean SNR of noisy signals are given in Table 1.

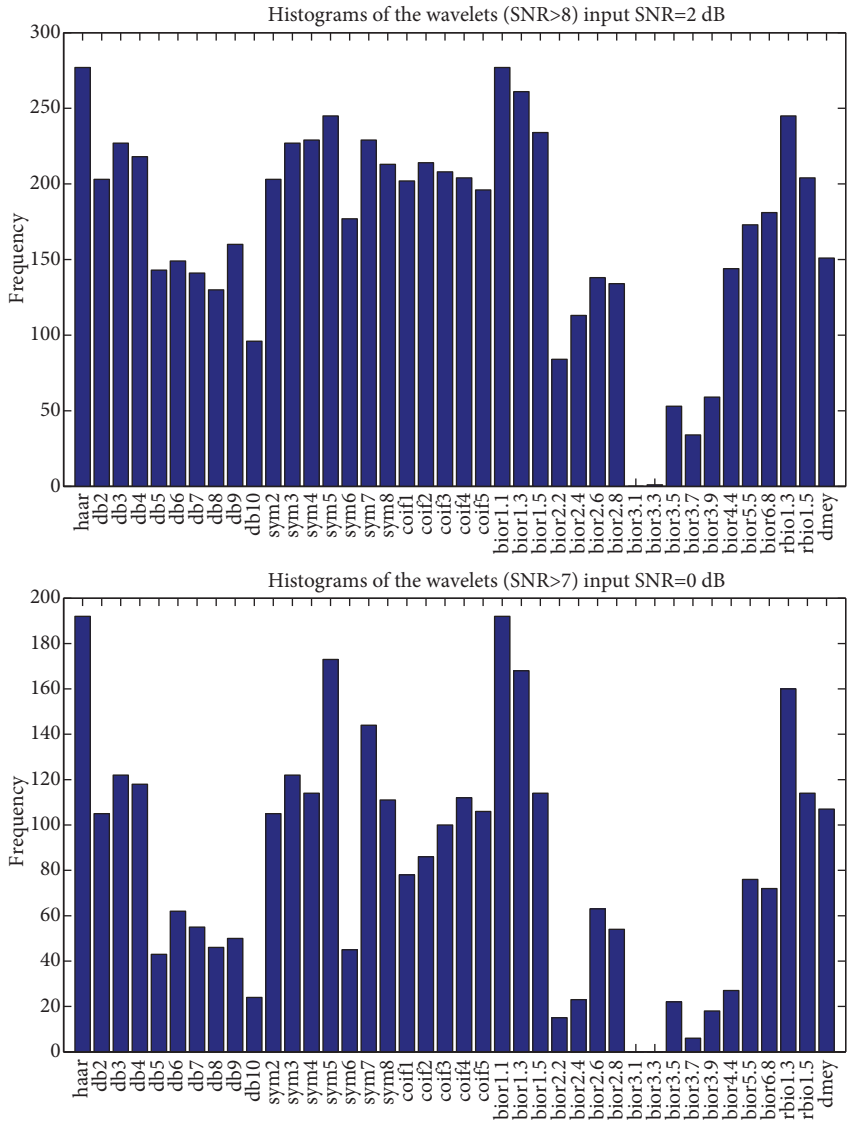

Figure 9. The histograms of wavelets whose SNR values are above the thresholds.

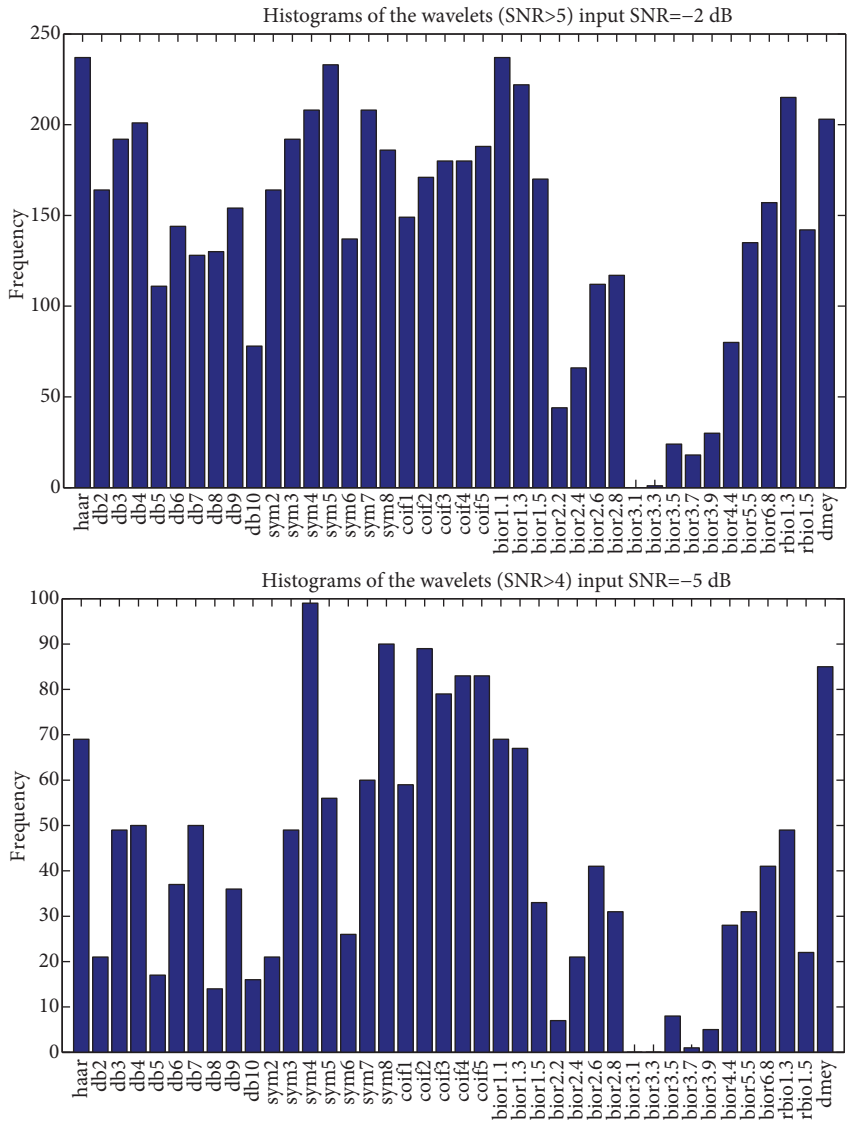

Figure 9. Continued.

Table 1. Optimum of wavelets, threshold rules, and threshold methods for different SNR values.

Input SNR values (dB)	Wavelet	Threshold rule	Threshold method
−7	sym4	Minimax	Soft
−5	sym4	Minimax	Soft
−2	bior1.1	SURE	Hard
0	bior1.1	SURE	Hard
+2	bior1.1	Minimax	Hard

The third and the last analysis on denoising sEMG signals was performed with a median filter. In this analysis, 3 different window-sized median filters (3, 5, and 7) were applied to the noisy synthetic signal separately. The best result was achieved when the window size was 3.

The performances of EMD- and DWT-based denoising and median filtering on –2 dB added synthetic sEMG signals are shown in Figures 10a, 10b, and 10c, and the mean SNR values of denoising techniques in contrast are shown in Table 2.

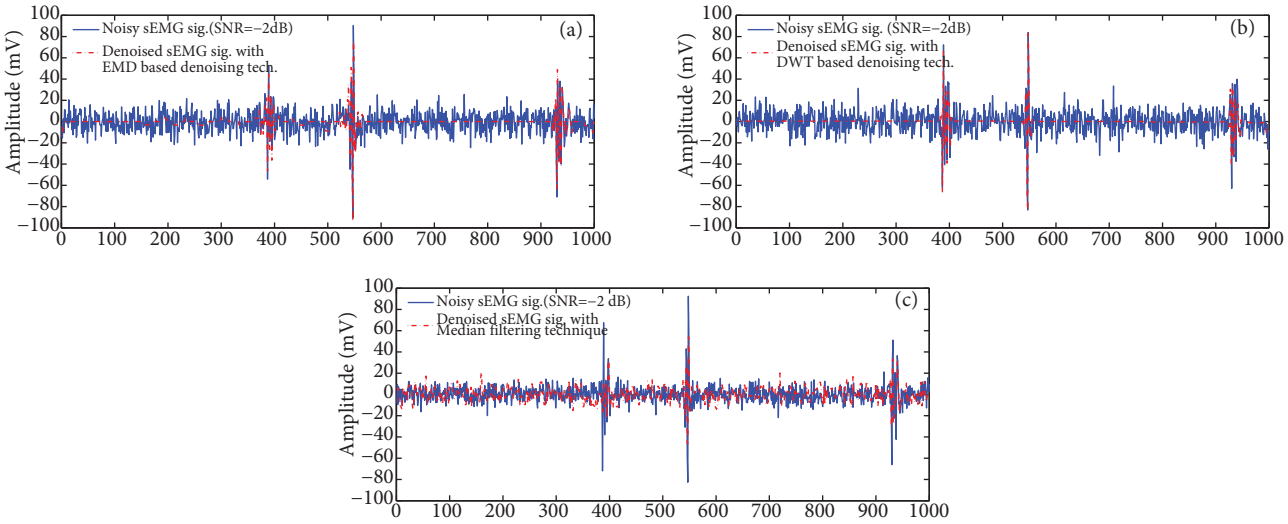

Figure 10. The results of the denoising techniques on the same –2 dB added synthetic sEMG signal: (a) EMD-based denoising, (b) DWT-based denoising (c) median filtering with a window size of 3.

Table 2. Mean SNR values of different denoising techniques.

Input SNR values (dB)	Mean SNR values (dB)		
	DWT	EMD	Median
–7	2.888	–1.112	–4.081
–5	3.968	1.415	–2.255
–2	6.274	3.790	0.122
0	7.071	5.356	1.555
+2	10.208	6.537	2.756

In the virtual representation of processes that were performed in this section, $-2dB$ AWGN added synthetic sEMG was preferred as an example signal source because $-2dB$ is the mid-value among the other noise levels.

3.2. Denoising results of real sEMG signals

The denoising performances of the filtering techniques on real signals can be observed visually. Figure 11 shows the performances of the filtering techniques. While filtering the real sEMG signal for DWT-based denoising, the bior1.1 wavelet function, the soft threshold method, and the minimax selection rule were used. For median filtering, the chosen window size was 3. For EMD-based denoising, the length of the noise windows was 100 samples, as in the synthetic signal.

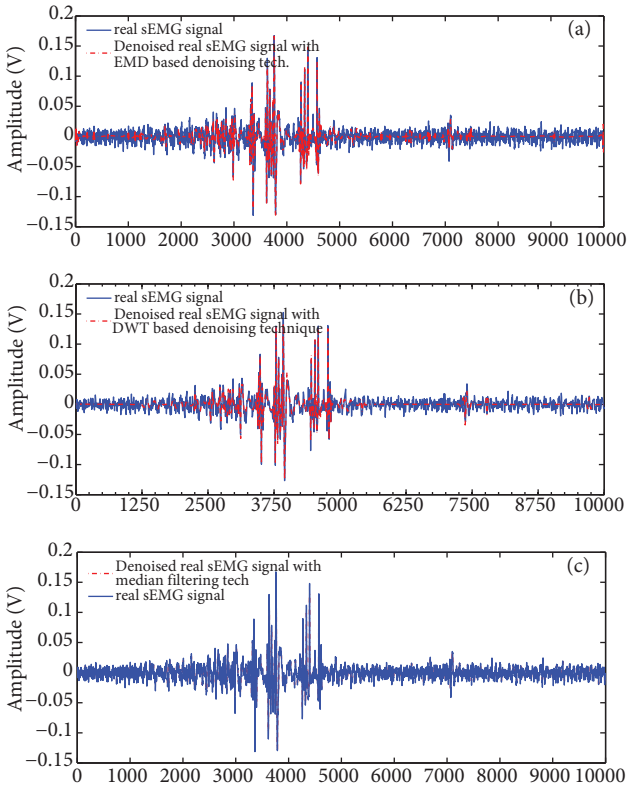

Figure 11. The performances of denoising techniques on the real sEMG signal: (a) EMD-based denoising, (b) DWT-based denoising, (c) median filtering with window size of 3.

4. Discussion

The performances of DWT, EMD, and median filter techniques in denoising sEMG signals are shown in Figure 12. Figure 12 reveals the maximum, minimum, and median SNR values of 30 times noise added sEMG signal. According to Table 1 and Figure 12, the wavelet-based denoising technique gives the best results, and the EMD-based denoising technique performs better than the median filter. This study also shows that wavelet-based and EMD-based denoising techniques protect the waveform, but a median filter may distort the signal. The only disadvantage of the wavelet-based denoising technique is that the user has to select a proper wavelet function, but this is not needed in the EMD-based denoising technique and the median filter. The major advantage of the EMD is that the basic functions are derived from the signal itself. When there is a need to use noising techniques in real-time processing, the median filter is more suitable than the other two techniques.

5. Conclusions

In this paper, three different denoising techniques were applied to synthetic and real sEMG signals while comparing their performances. The wavelet functions that are suitable for denoising sEMG signals were discussed as well. The results showed that the wavelet-based denoising technique outperforms EMD-based denoising and median filtering. In high-noise environments, sym4, sym8, coif2, and coif5 wavelet functions and the soft threshold method give the best results, whereas in less noisy environments bior1.1, haar, and sym5 wavelet functions and the hard threshold method give the best results. Minimax and SURE selection rules performed better than the hybrid and universal threshold rules.

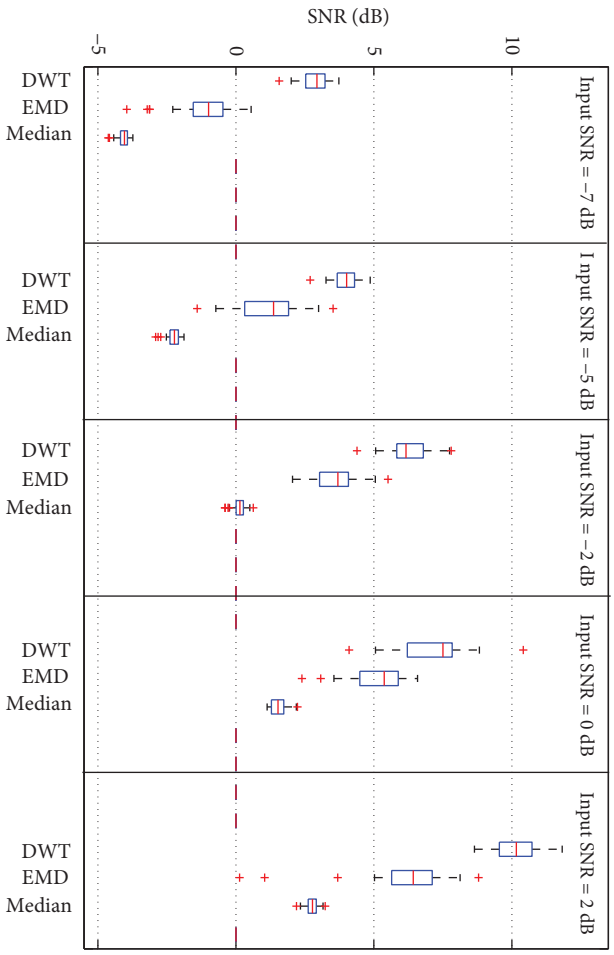

Figure 12. Performance comparison of DWT, EMD and median filter techniques on 5 different levels of a noise-added synthetic sEMG signal.

References

[1] N. Bu, M. Okamoto, T. Tsuji, "A hybrid motion classification approach for emg-based human-robot interfaces using Bayesian and neural networks", IEEE Transactions on Robotics, Vol. 25, pp. 502–511, 2009.

[2] O. Fukuda, J. Kim, I. Nakai, Y. Ichikawa, "EMG control of a pneumatic 5-fingered hand using a Petri net", Artificial Life and Robotics, Vol. 16, pp. 90–93, 2011.

[3] G.G. Gutiérrez, C.B. López, F. Navacerrada, A.M. Martínez, "Use of electromyography in the diagnosis of inflammatory myopathies", Reumatología Clínica (English edition), Vol. 8, pp. 195–200, 2012.

[4] U. Baspinar, H.S. Varol, V.Y. Senyurek, "Performance comparison of artificial neural network and Gaussian mixture model in classifying hand motions by using sEMG signals", Biocybernetics and Biomedical Engineering, Vol. 33, pp. 33–45, 2013.

[5] B. Karlık, "Differentiating type of muscle movement via AR modeling and neural network classification", Turkish Journal of Electrical Engineering, Vol. 7, pp. 45–52, 1999.

[6] E. Huigen, A. Peper, C. Grimbergen, "Investigation into the origin of the noise of surface electrodes", Medical and Biological Engineering and Computing, Vol. 40, pp. 332–338, 2002.

[7] C.J. De Luca, L. Donald Gilmore, M. Kuznetsov, S.H. Roy, "Filtering the surface EMG signal: movement artifact and baseline noise contamination", Journal of Biomechanics, Vol. 43, pp. 1573–1579, 2010.

[8] M.B.I. Reaz, M. Hussain, F. Mohd-Yasin, "Techniques of EMG signal analysis: detection, processing, classification and applications", Biological Procedures Online, Vol. 8, pp. 11–35, 2006.

[9] N. Gallagher, G. Wise, "A theoretical analysis of the properties of median filters", IEEE Transactions on Acoustics, Speech and Signal Processing, Vol. 29, pp. 1136–1141, 1981.

[10] T. Nodes, N. Gallagher, "Median filters: some modifications and their properties", IEEE Transactions on Acoustics, Speech and Signal Processing, Vol. 30, pp. 739–746, 1982.

[11] C.F. Jiang, S.L. Kuo, "A comparative study of wavelet denoising of surface electromyographic signals", 29th Annual International IEEE Conference on Engineering in Medicine and Biology Society, pp. 1868–1871, 2007.

[12] A.O. Andrade, S. Nasuto, P. Kyberd, C.M. Sweeney-Reed, F. Van Kanijn, "EMG signal filtering based on empirical mode decomposition", Biomedical Signal Processing and Control, Vol. 1, pp. 44–55, 2006.

[13] A. Karagiannis, P. Constantinou, "Noise-assisted data processing with empirical mode decomposition in biomedical signals", IEEE Transactions on Information Technology in Biomedicine, Vol. 15, pp. 11–18, 2011.

[14] M. Kania, M. Fereniec, R. Maniewski, "Wavelet denoising for multi-lead high resolution ECG signals", Measurement Science Review, Vol. 7, pp. 30–33, 2007.

[15] N. Chatlani, J.J. Soraghan, "EMD-based filtering (EMDF) of low-frequency noise for speech enhancement", IEEE Transactions on Audio, Speech and Language Processing, Vol. 20, pp. 1158–1166, 2012.

[16] F. Damiani, A. Maggio, G. Micela, S. Sciortino, "A method based on wavelet transforms for source detection in photon-counting detector images. I. Theory and general properties", The Astrophysical Journal, Vol. 483, pp. 350–369, 1997.

[17] B. Karlık, Y. Koçyiğit, M. Korürek, "Differentiating types of muscle movements using a wavelet based fuzzy clustering neural network", Expert Systems, Vol. 26, pp. 49–59, 2009.

[18] Z.N. Li, Z.Z. Luo, "Spatial correlation filtering based on wavelet transformation application to EMG de-noising", Dianzi Xuebao (Acta Electronica Sinica), Vol. 35, pp. 1414–1418, 2007.

[19] B. Dogan, I. Goker, M.B. Baslo, H. Erdal, Y. Ulgen, "Interface design for automation of the scanning EMG method", Conference Proceedings of the 14th National Biomedical Engineering Meeting, BIYOMUT, pp. 1–4, 2009.

[20] M.A. Kabir, C. Shahnaz, "Denoising of ECG signals based on noise reduction algorithms in EMD and wavelet domains", Biomedical Signal Processing and Control, Vol. 7, pp. 481–489, 2012.

[21] D. Safieddine, A. Kachenoura, L. Albera, G. Birot, A. Karfoul, A. Pasnicu, A. Biraben, F. Wendling, L. Senhadji, I. Merlet, "Removal of muscle artifact from EEG data: comparison between stochastic (ICA and CCA) and deterministic (EMD and wavelet-based) approaches", EURASIP Journal on Advances in Signal Processing, Vol. 2012, p. 127, 2012.

[22] H.R. Marateb, EMGLAB Signals, 2011, available at http://www.emglab.net/emglab/Signals/signals.php.

[23] N.E. Huang, Z. Shen, S.R. Long, M.C. Wu, H.H. Shih, Q. Zheng, N.C. Yen, C.C. Tung, H.H. Liu, "The empirical mode decomposition and the Hilbert spectrum for nonlinear and non-stationary time series analysis", Proceedings of the Royal Society of London Series A, Vol. 454, pp. 903–995, 1998.

[24] D.L. Donoho, "De-noising by soft-thresholding", IEEE Transactions on Information Theory, Vol. 41, pp. 613–627, 1995.

[25] S. Mallat, A Wavelet Tour Of Signal Processing, 3rd ed., Amsterdam, Elsevier, 2002.

[26] P.S. Addison, The Illustrated Wavelet Transform Handbook, London, Institute of Physics Publishing, 2002.

[27] A. Phinyomark, C. Limsakul, P. Phukpattaranont, "A comparative study of wavelet denoising for multifunction myoelectric control", International Conference on Computer and Automation Engineering, ICCAE, pp. 21–25, 2009.

[28] S. Li, G. Liu, Z. Lin, "Comparisons of wavelet packet, lifting wavelet and stationary wavelet transform for denoising ECG", 2nd IEEE International Conference on Computer Science and Information Technology, ICCSIT, pp. 491–494, 2009.

[29] J. Gao, H. Sultan, J. Hu, W. W. Tung, "Denoising nonlinear time series by adaptive filtering and wavelet shrinkage: a comparison", IEEE Signal Processing Letters, Vol. 17, pp. 237–240, 2010.

[30] S. Poornachandra, "Wavelet-based denoising using subband dependent threshold for ECG signals", Digital Signal Processing, Vol. 18, pp. 49–55, 2008.

[31] R. Q. Quiroga, H. Garcia, "Single-trial event-related potentials with wavelet denoising", Clinical Neurophysiology, Vol. 114, pp. 376–390, 2003.